SIMULATING REALISTIC EARTHQUAKE GROUND MOTIONS IN REGIONS OF DEEP SEDIMENTARY BASINS

ROBERT W. GRAVES

Woodward Clyde Federal Services
566 El Dorado St., Pasadena, CA 91101
tel: (818) 449-7650 / fax: (818) 449-3536 / email: rwgrave0@wcc.com

ABSTRACT

We have developed a workstation based numerical simulation technique to model seismic wave propagation in arbitrarily complex 3D elastic media. The technique uses a staggered-grid finite-difference approach and is capable of generating highly accurate results. Due to the substantial storage requirements needed for the 3D finite-difference models, we have designed a memory optimization algorithm which reduces system overhead to a manageable level and allows the code to be implemented on a workstation platform. The method has been successfully applied to model the long-period (T>1 sec) ground motions for several recent earthquakes, including the 1987 Whittier Narrows, 1994 Northridge, and 1995 Kobe events. This workstation based technique provides an efficient and practical method to calculate the seismic response for large-scale, 3D geologic models.

KEYWORDS

Finite-difference simulations, workstation, basin response, Whittier Narrows, Kobe

INTRODUCTION

Many urban regions, including Los Angeles and Seattle in the United States, Osaka and Tokyo in Japan, and Mexico City in Mexico are located above large sedimentary basins. The conventional engineering approach to estimate earthquake ground motions is to assume that the near-surface geology can be characterized by a horizontally stratified medium, and that only the shallowest few tens of meters influence the ground motion characteristics. However, this simple approach may significantly underestimate the amplitudes and durations of strong ground motions, especially at periods of about one second and longer, where seismic energy can become trapped within the dipping sedimentary layers due to critical reflections that are set up at the edges of the basin. These effects are due to the geometry of the interface between the sedimentary materials and the underlying crystalline rocks, and cannot be explained by the shallow soil profile alone. Many elements of the urban infrastructure, such as bridges, multi-story buildings, dams and storage tanks, are susceptible to long-period ground motions.

Recently, much interest has been generated concerning the simulation of earthquake ground motions in realistic 3D geologic structures. The most general simulation methods are grid based techniques, which typically require substantial computational resources in order to produce results of practical interest. One way to handle this computational demand is to utilize the resources of a multi-processor supercomputer. However, these types of machines are extremely expensive and their use can require a significant amount

of software development. As an alternative, we have developed a 3D simulation technique which can be run on a conventional desktop workstation (Graves, 1995). Our technique uses a staggered-grid finite-difference scheme to model the first-order elastodynamic equations of motion. The scheme is accurate to 4th order in space and 2nd order in time, is applicable to arbitrarily heterogeneous 3D elastic media, and can model the response of numerous types of sources, including extended fault rupture. The algorithm is designed with a memory optimization technique which reduces system overhead to a manageable level and allows the code to be implemented on a workstation platform.

By using a finite-difference approach, we are able to compute the complete wave field on a fine spatial mesh throughout a large region of interest. This capability has the potential to greatly enhance the microzonation of urban regions located on sedimentary basins. Instead of obtaining ground motion estimates at a set of discrete locations using local flat layered geological models, which may be inaccurate because they do not account for the effects of the basin structure, we are able to calculate the seismic wave field throughout the urban region, with the ground motion characteristics at each location incorporating the effects of the laterally varying geologic structure in its vicinity. We have tested our procedure for calculating ground motions in basins against ground motions recorded in the Marina District in San Francisco during aftershocks of the 1989 Loma Prieta earthquake, in the Eel River Valley during the 1992 Cape Mendocino earthquake, in the west Los Angeles and Santa Monica regions during the 1994 Northridge earthquake, at sites throughout the Los Angeles region during the 1987 Whittier Narrows earthquake, and at sites in the Kobe and Osaka area during the 1995 Kobe earthquake. In all of these cases, we have found that the recorded ground motions can be better explained using basin structures rather than using simple flat layer models.

BASIN RESPONSE AT LONG PERIODS (T > 1 SEC)

At long-periods (T > 1 sec), the strong ground motions in the epicentral region of large earthquakes are controlled primarily by deterministic features of the earthquake source and seismic wave propagation. Recent studies have shown the usefulness of synthetic seismogram modeling techniques to match the recorded data and develop heterogeneous-slip rupture models of past earthquakes (eg., Mendoza and Hartzell, 1988). In addition, earthquakes often occur in regions of complicated geology and wave propagation through these variable geologic structures can significantly affect the observed strong ground motions, particularly at periods greater than 1 sec. For example, Vidale and Helmberger (1988) demonstrated that the long-period (1-10 sec) strong ground motions recorded in the Los Angeles region during the 1971 San Fernando earthquake were dominated by surface wave energy that was generated by seismic waves trapped within the San Fernando and Los Angeles basins.

In the conventional engineering approach to estimating site response, effects due to near surface geology are approximated using a 1D model of the structure beneath the site. This method is useful for estimating impedance amplification effects, but it cannot reproduce the effects of focusing, resonance and extended duration of shaking that are observed when the near surface geology is laterally varying. This situation is illustrated schematically in Figure 1. Using a 1D model of the near surface geology, a wave incident from below may resonate but cannot be trapped in the near surface sedimentary layers (top left panel, Figure 1). However, small departures from horizontal layering can result in the trapping of waves within the structure. As body waves enter a basin through its thickening margin, total internal reflection of energy can develop, as illustrated in the top right panel of Figure 1. The waves become trapped as surface waves in the basin and propagate across the basin until they reach the thinning edge where they develop pre-critical angles of incidence and escape as body waves. The lower panels of Figure 1 show a synthetic wave field example which clearly demonstrates these effects. Due to the combined effects of impedance amplification and trapping of energy, the basin generated surface waves can become quite large, being comparable to or larger than the direct wave in this simulation (Figure 1c). In contrast, the flat layer (1D) model response will always be dominated by the direct arriving energy (Figure 1b).

The map in Figure 2 shows the location of CSMIP strong motion stations in the Los Angeles basin region which recorded the Whittier Narrows mainshock. This event occurred on the northeast flank of the basin at a depth of about 15 km. We have simulated the strong motions from this event using the finite-fault source model of Hartzell and Iida (1990) and incorporating the 3D basin structure depicted in Figure 2. The wave field simulation technique is based on the 3D elastic, staggered-grid finite-difference modeling algorithm discussed in Graves (1995). In this simulation, the numerical model represents a block of crust covering an area 50 km × 50 km and extending to a depth of 18 km. Using a grid spacing of 0.2 km, we obtain accurate results up to 1 Hz in the lowest velocity regions of the model (v_s = 1.0 km/sec). The calculation was run for 3000 time steps with a time spacing of 0.01 sec, resulting in a ground motion simulation of 30 sec duration following the earthquake origin time. The model grid consists of over 5.6 × 10^6 nodes and the computation required 33 hours of CPU time on a Sun Workstation.

The top panel of Figure 3 displays the radial and tangential components of ground velocity recorded along a profile of stations across the LA basin. Many of the basin recordings (eg., down, lbrp, hadb) show a large long-period pulse of energy arriving about 7-8 seconds after the direct shear wave (labelled SS in Figure 3). This pulse is most clearly seen on the tangential component of motion for stations located due south of the epicenter. Scrivner and Helmberger (1994) explain the late arriving pulse as a bouncing S wave that is trapped by the dipping layers of the basin sediments. The response computed for these sites using the 3D modeling technique is displayed in the lower panel of Figure 3. In general, the ground motions are reproduced quite well using the 3D model, and furthermore, the 3D simulation is able to accurately predict the occurrence of the basin generated phase (SS).

Figure 4 shows wave field time slices of the east-west component of ground velocity for the 3D simulation of the Whittier Narrows event. These time slices clearly illustrate the developing complexity of the ground motions as the waves propagate through the basin structure. In the near-source region, the primary effect of the basin structure is to delay the arrival of energy which propagates through the low velocity sediments (t=6-8 sec). At t=10 sec, increasing complexity in the wave field begins to emerge, with the generation of surface wave energy at the northern margin of the Los Angeles basin. By t=12 sec, three distinct arrivals are seen; the direct S-wave in the southwesternmost portion of the basin, which has traveled *beneath* the deepest portion of the basin, the direct S-wave in the middle portion of the basin, which has propagated *upwards through* the basin sediments, and the basin generated surface wave, which is visible in the northern portion of the basin. The complexity in the wave field is due to the bending, refraction, and reflection of energy by the dipping layers of the basin structure. In this manner, the basin effectively forms a shadow zone for the direct S wave at sites in the southern portion of the basin, while creating a hot spot or bright zone by focusing energy in the middle portion of the basin. For later times (t=16 sec), the wave field becomes even more complex due to the effects of the basin structure, and, in fact, all of the significant energy seen in these time slices is due to basin generated phases. In addition, although most of the energy is still propagating outward from the source (ie., backscattered energy is negligible), there is very little azimuthal coherency to the wave field.

Furthermore, the development of the basin generated surface wave (SS phase) is easily seen by viewing the time sequence of depth cross-sections shown in Figure 4. The evolution of this phase is as follows. At t=8 sec the upward propagating, direct S wave from the source is reflected downward from the free-surface. At t=10 sec, this downward traveling energy hits the dipping layers of the sediment/basement interface at or beyond critical incidence and is strongly reflected back towards the surface. By t=12 sec, this wave energy has become trapped between the free-surface and the basin bottom and is propagating in a nearly horizontal direction within the sediments of the basin. This situation is analogous to the schematic ray diagram shown in the top right panel of Figure 1.

DISCUSSION AND CONCLUSIONS

The preceding example clearly illustrates the complexity in ground motion response that is created by the 3D structure of the LA basin. In addition, it is evident that the spatial variability of ground motions, particularly for the basin generated phases, is strongly influenced by lateral variations in geologic structure. These features are characteristic of the long-period ground motions which have been observed in basin regions for a number of recent earthquakes, and by using these data, we have been able to validate our 3D numerical simulation technique. While the simulation of 3D elastic wave fields in realistic geologic media can be computationally intensive, it does not represent an unreachable goal. This fact is illustrated by the data in Table 1 which summarizes the model parameters and CPU run times for two recently completed simulations. These simulations were run on our current workstation platform which consists of a Sun Sparcstation with a 125 MHz processor, 192 Mbytes of core memory, and a 2 Gbyte hard disk.

Table 1. Model parameters and CPU times for 3D FD workstation simulations.

	Whittier Narrows	Kobe
Model dimensions (nx×ny×nz)	250×250×90	400×300×120
Total time steps	3000	6000
Grid spacing (km)	0.2	0.2
Time step (sec)	0.01	0.015
Minimum velocity (km/sec)	1.0	0.55
Maximum simulated frequency (Hz)	1.0	0.5
Model size (total grid points)	5.625×10^6	1.44×10^7
CPU per time step (sec)	40	104
Total CPU (hours)	33	175

To date, the simulation of the 1995 Kobe earthquake is the largest that we have conducted. The model consists of 1.44×10^7 grid points and required 104 sec of CPU to perform each time update, for a total of 175 CPU hours to produce 90 sec (6000 time steps) of simulated motions. This model is comparable in size to the largest calculations performed using supercomputer technology (eg., Olsen et al., 1995), yet requires only a factor of 6 more CPU time when computed using the workstation based wave field simulation technique discussed in this paper. The workstation approach thus offers an efficient and practical way in which we can to calculate the expected nature of long period ground motions for future earthquakes in regions of complex geology.

REFERENCES

Graves, R. W. (1995). Simulating wave propagation in 3D elastic media using staggered-grid finite-differences, submitted to *Bull. Seism. Soc. Am.*.

Hartzell, S. and M. Iida (1990). Source complexity of the 1987 Whittier Narrows, California, earthquake from the inversion of strong motion records, *J. Geophys. Res.*, 95, 12,475-12,485.

Mendoza, C. and S Hartzell (1988). Aftershock patterns and main shock faulting, *Bull. Seism. Soc. Am.*, 78, 1438-1449.

Olsen, K. B., R. J. Archuleta, and J. R. Matarese (1995). Magnitude 7.75 earthquake on the San Andreas fault: three-dimensional ground motion in Los Angeles, *Science*, in press.

Scrivner, C. W. and D. V. Helmberger (1994). Seismic waveform modeling in the Los Angeles basin, *Bull. Seism. Soc. Am.*, 84, 1310-1326.

Vidale, J. E. and D. V. Helmberger (1988). Elastic finite-difference modeling of the 1971 San Fernando, California earthquake, *Bull. Seism. Soc. Am.*, 78, 122-141.

Flat Layer Case (1D)

Basin Case

V_2 $(V_2 > V_1)$

V_2 $(V_2 > V_1)$

$i < i_c$ (critical angle)
energy resonates, but is not trapped

$i > i_c$ (critical angle)
energy is trapped in top layer

(a)

rock site (1D)

(c)

basin profile (2D)
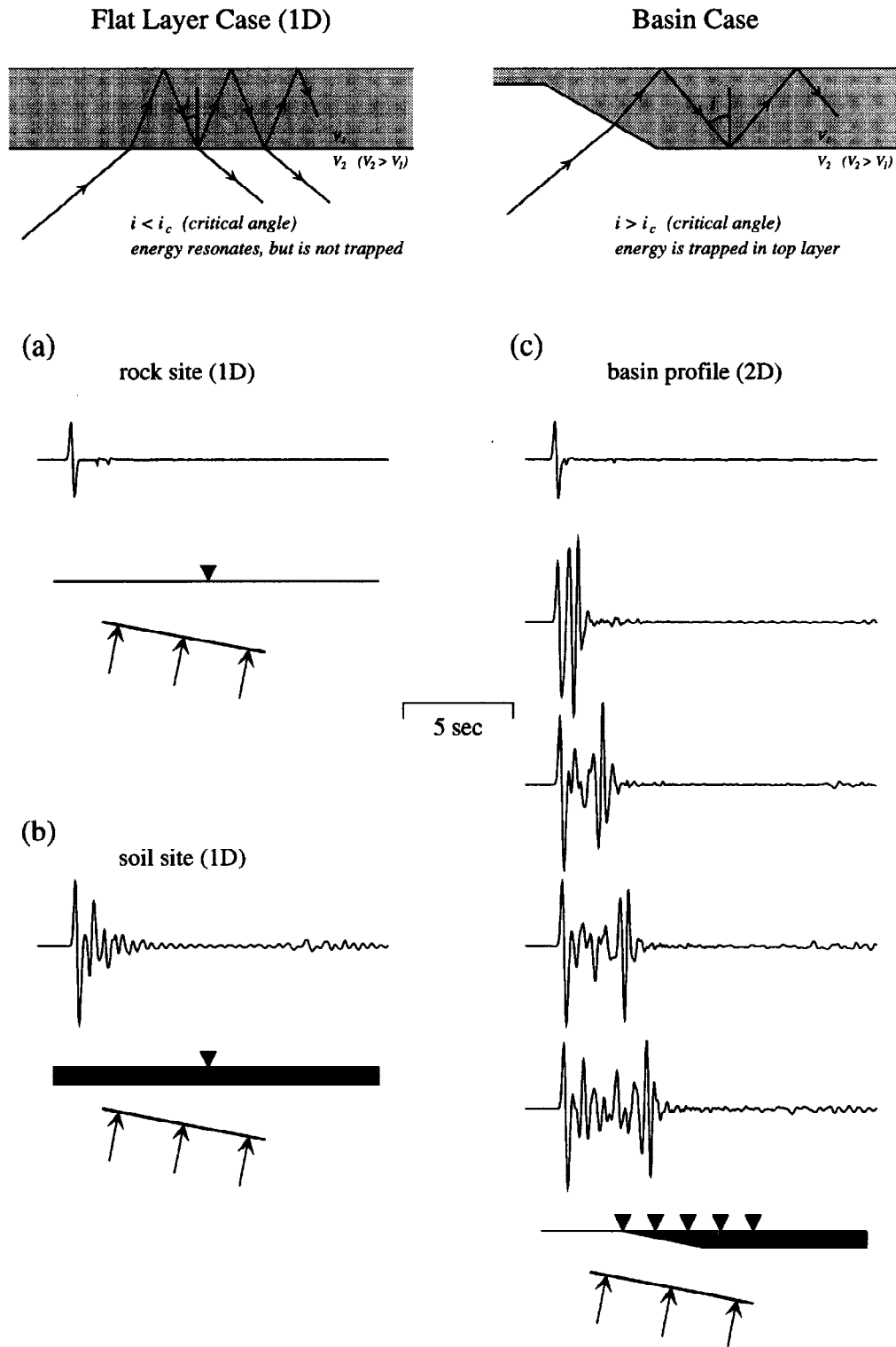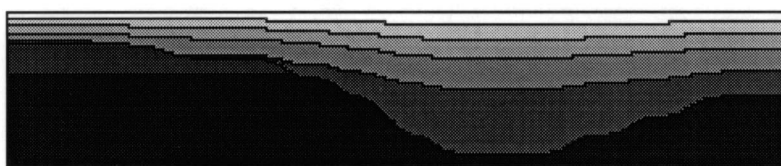
5 sec

(b)

soil site (1D)

Figure 1: Top panels show schematic ray diagrams illustrating the trapping mechanism of waves within sedimentary basins. The bottom panels show finite-difference SH velocity synthetics for (a) a rock site, (b) a soil site, and (c) a profile of stations across a basin margin. The basin profile shows the development of a large amplitude surface wave which is generated at the basin margin and then propagates into the basin with a slow apparent velocity. Due to post critical reflection at the sediment/baserock interface, this late arriving energy is effectively trapped within the basin sediments.

1987 Whittier-Narrows Earthquake
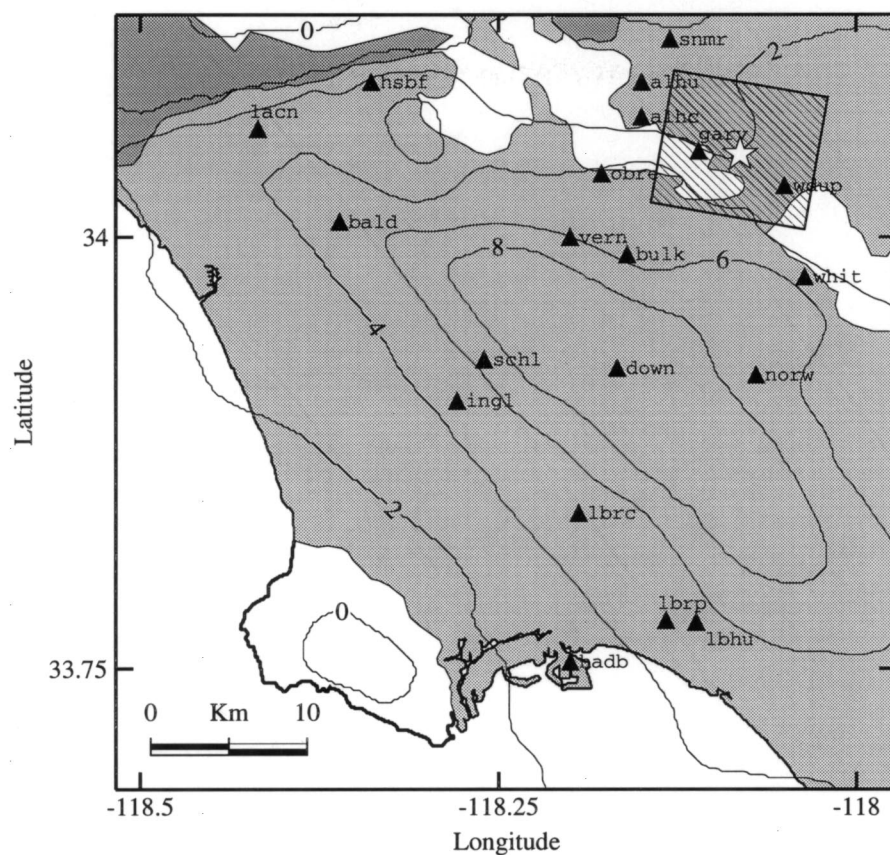
Velocity Model Cross-Sections

east-west cross-section at station down

Vp	Vs	den	Qs
2.00	1.00	1.40	50
2.40	1.30	1.60	100
3.10	1.70	1.90	200
3.50	2.00	2.00	350
3.60	2.10	2.20	400
4.30	2.50	2.20	500
5.50	3.20	2.50	750
6.30	3.60	2.70	1000

north-south cross-section at station down
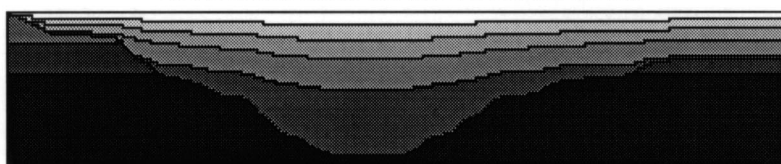
no vertical exaggeration   *horizontal scale*

0   km   10.0

Figure 2: Top panel shows location of CSMIP strong motion recording sites in the Los Angeles area for the 1987 Whittier Narrows earthquake. The epicenter of the event is indicated by the open star, and depth to basement contours (in km) are also shown on the map. Bottom panels show cross-sections through this structure indicating the distribution of seismic velocity and density in the Los Angeles basin. The maximum depth of the basin is around 9 km.

Observed Velocity Records
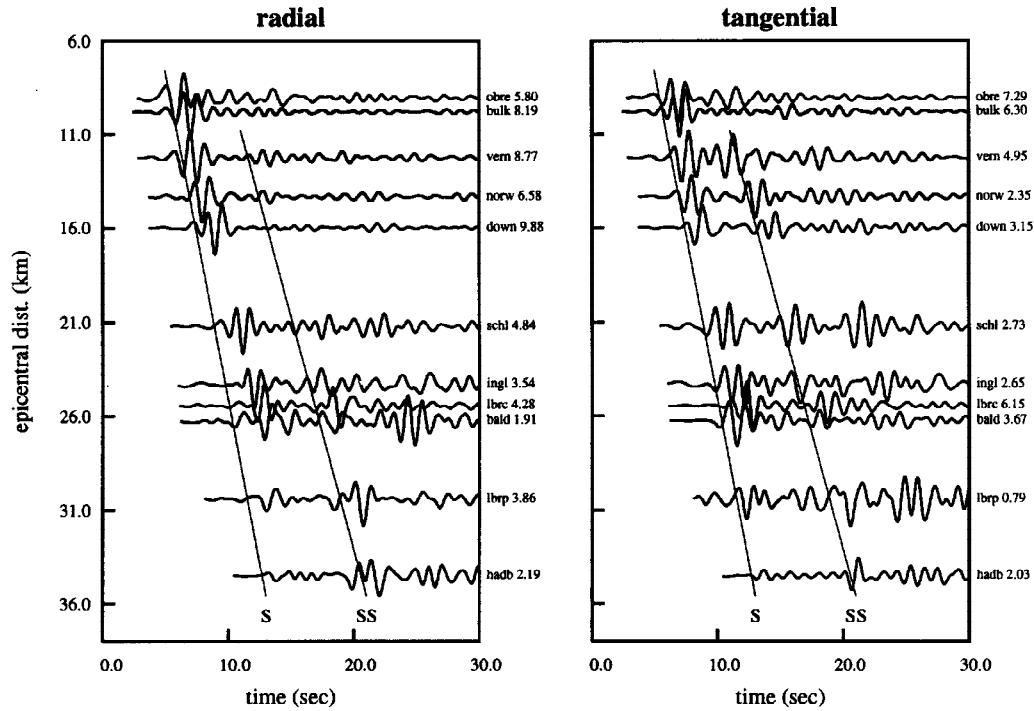
radial

tangential

3D Basin Model Simulation
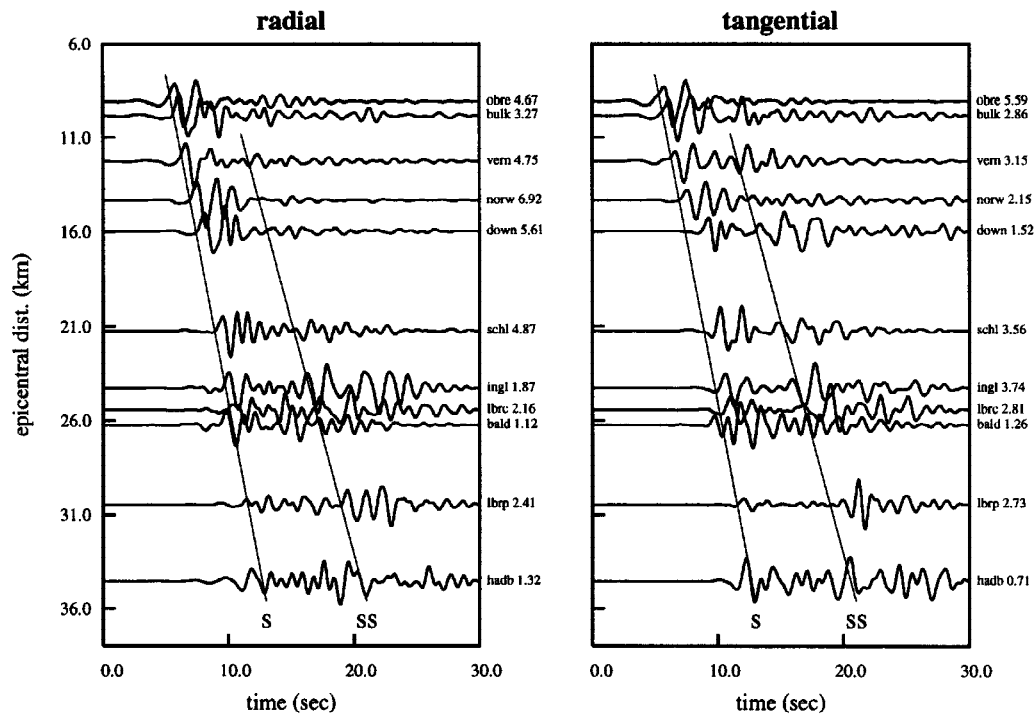
radial

tangential

Figure 3: Recorded (top) and simulated (bottom) horizontal ground velocity time histories for the Whittier Narrows earthquake. Both sets of time histories have been rotated into radial and tangential components relative to the earthquake epicenter then low-pass filtered at 1Hz. The timing lines indicate the direct S wave (S) and the bouncing S wave trapped by the basin structure (SS). Using the 3D simulation model, we are able to generate synthetic time histories which are quite similar to the recorded data, including the accurate reproduction of the SS phase. The occurrence of this phase is not predicted when using a plane-layer (1D) model to represent the basin structure.
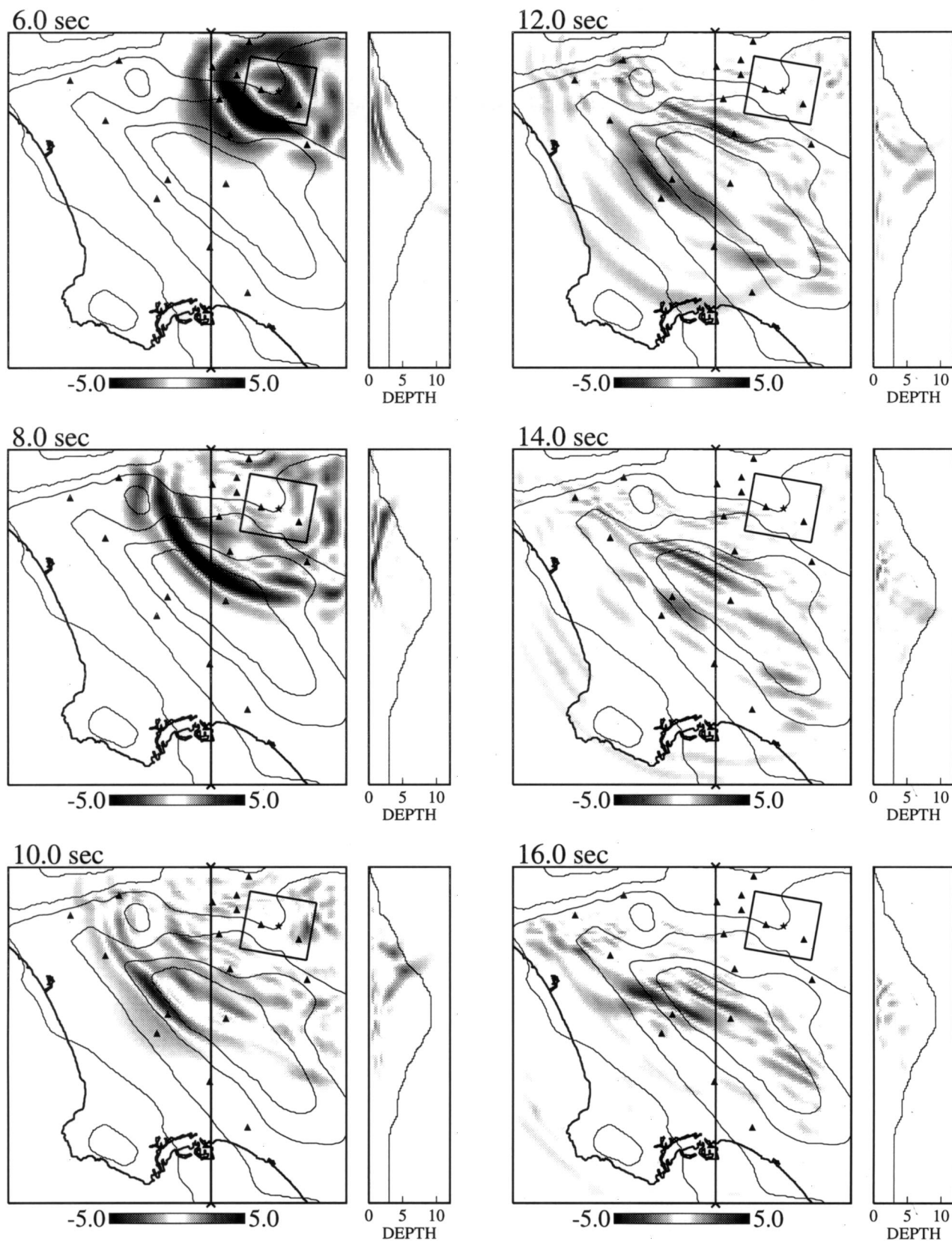
Figure 4: Wave field snapshots of the east-west component of ground velocity for the 3D Whittier Narrows earthquake simulation. Each panel has a map view and a north-south cross-section taken along the profile line indicated on the map. Time slices are at t=6 sec (top left), t=8 sec (middle left), t=10 sec (bottom left), t=12 sec (top right), t=14 sec (middle right), and t=16 sec (bottom right).